Phase diagram of a three-dimensional anisotropic long-range Ising model versus temperature and magnetic field

1992 J. Phys.: Condens. Matter 4 5921

(http://iopscience.iop.org/0953-8984/4/27/011)

J. Phys.: Condens. Matter 4 (1992) 5921–5946. Printed in the UK

Phase diagram of a three-dimensional anisotropic long-range Ising model versus temperature and magnetic field

L M Floría†, P Quémerais‡ and S Aubry§

† Instituto de Ciencia de Materiales de Aragón (CSIC-UZ) and Departamento de Física de la Materia Condensada, Facultad de Ciencias, Universidad de Zaragoza, 50009 Zaragoza, Spain

‡ Institut des Matériaux, UMR 100, 2 Rue de la Houssinière, 44072 Nantes Cédex, France

§ Laboratoire Léon Brillouin||, CEN Saclay, 91191 Gif-sur-Yvette Cédex, France

Received 25 November 1991, in final form 20 March 1992

Abstract. The phase diagram of a three-dimensional Ising model in a magnetic field with commensurate and incommensurate phases is studied at low temperature within a mean-field approximation. This analysis was motivated by problems in condensed matter physics concerning, for example, bipolaronic charge-density waves, neutral-to-ionic transitions in organic salts, staging in intercalation compounds, magneto-elastic materials, stacking in discotic liquid crystals, etc. The interactions between the Ising spins are long-range exponentially decaying, and are antiferromagnetic in one direction and ferromagnetic in the perpendicular planes.

The ground state of this model is known to be a commensurate or an incommensurate structure with a wavevector that varies as a complete devil's staircase as a function of the magnetic field. Provided some conditions hold on the model parameters, we prove rigorously that, for small enough temperature, the mean-field variational form of the model still yields a minimum that is a commensurate or an incommensurate structure, the wavevector of which also varies as a complete devil's staircase as a function of the magnetic field or temperature.

The explicit computation of the phase diagram is done by using two methods that are consistent with one another: the first is based on the numerical analysis of a transfer matrix at zero degrees kelvin; the second is based on an approximation valid at low temperature, which allows one to map this mean-field model onto a Frenkel–Kontorova model. This second method yields an analytical expression for the transition lines of the phase diagram.

1. Introduction

This paper is devoted to the mean-field analysis at low temperature of the phase diagram of an anisotropic Ising model in a magnetic field. Unlike the well known ANNNI model, this model can exhibit commensurate and truly incommensurate ground states. Our main purpose is to obtain some useful qualitative information on the thermal behaviour and the wavevector variation at low temperature of non-analytic incommensurate phases.

Before introducing the model, let us first recall the characteristic properties of non-analytic incommensurate structures. They are characterized by the fact that

|| Laboratoire Commun CEA–CNRS.

0953-8984/92/275921+26$04.50

their microscopic configurations are discontinuous functions of their phase. As a physical consequence, the incommensurate modulations of these structures are intrinsically pinned to the lattice and are phase-defectible (i.e. they admit phase defects as metastable configurations; analytical incommensurate structures being, on the contrary, undefectible). Another consequence is that the phonon spectrum associated with the phase fluctuations (phason) exhibits a strictly non-zero gap. At low temperature the relevant excitations that describe the thermodynamics of the system are not these phonon modes but are those metastable configurations which correspond to random distributions of phase defects. The thermal fluctuations of these metastable configurations contribute to the dynamical response function as a central peak with a narrow width in frequency.

It has been shown that the non-analytic incommensurate phases are well described by an effective Hamiltonian defined on discrete variables instead of continuous atomic coordinates. These discrete variables could be, for example, integers (as in the Frenkel–Kontorova model at $d \geqslant 2$ dimensions [1]) but can often be reduced to Ising (or pseudo-spin) variables as for the one-dimensional (1D) Frenkel–Kontorova model and for the bipolaronic structures of many coupled electron–phonon models [2]. Within a general framework, the nature of the site variable (Ising spin, integer or else), which has to be used to describe the metastable defect configurations, is determined by the coding sequences, which have to be used at the 'anti-integrable' limit of the considered model [3]. This justifies very generally why Ising spin Hamiltonians are appropriate for describing non-analytic incommensurate phases.

The effective Ising Hamiltonian that describes the thermodynamical behaviour of the non-analytic incommensurate phases at low temperature depends sharply on the initial model. It is generally quite complex, involving not only pair interactions but three-spin, four-spin, ... interactions, which become more and more essential when approaching the transition by breaking of analyticity (TBA) [4]. Sufficiently far away from the TBA, we can drop the multi-spin interactions beyond order 2. There are also special choices of the model for incommensurate structures, where an effective Hamiltonian with only one- and two-spin interactions can be explicitly obtained. However, these models are somewhat pathological at low coupling since they cannot exhibit any analytic incommensurate phase and thus any TBA. This situation occurs for example in the 1D Frenkel–Kontorova model with a piecewise parabolic periodic potential and harmonic springs [5]. We then obtain a Hamiltonian that is an Ising model with exponentially decaying long-range interactions with an external magnetic field. The thermodynamical properties of this model were studied in detail in [6]. However, although this 1D model exhibits a hierarchy of crossover temperatures when T goes to zero, it does not exhibit any true phase transition with ordered phases. The crossover temperature corresponds only to smooth changes in the thermodynamical behaviour and in the spin correlations.

In this paper, we analyse the phase diagram of a three-dimensional (3D) version of this 1D model. This 3D model consists of 1D chains with the same Hamiltonian as in [6]. We introduce phenomenologically a ferromagnetic coupling J between the chains, which might not be realistic in many physical situations but is simpler in a first approach of the 3D case. The main advantage of this choice is that the mean-field variational form of this 3D model easily reduces to that of a 1D model. Nevertheless, the results obtained should shed some light on the possible behaviour of 3D models.

This Ising Hamiltonian is

$$H = \sum_{i,j} \left(\sum_{(n>0)} J(n) S_{i,j} S_{i+n,j} \right) - J \sum_{\delta} S_{i,j} S_{i,j+\delta} - H S_{i,j} \qquad (1.1)$$

where (i,j) labels a site in a 3D cubic lattice (i for the z direction and $j = (j_x, j_y)$ for the perpendicular directions) and δ is a vector in the xy plane connecting in-plane interacting sites (which we will assume to be nearest neighbours); H is the external magnetic field, $J(>0)$ is the interaction constant within the xy planes, and $J(n)$ is the (decaying) interaction constant between nth neighbouring pseudo-spins in the chains along the z direction. For convenience, we choose for $J(n)$ the explicit form

$$J(n) = D\eta^{|n|} \qquad (1.2)$$

with D and $\eta\,(0 \leqslant \eta \leqslant 1)$ some constants.

A particularly important issue, regarding qualitative physical predictions based on the analysis of this model, concerns the bipolaronic charge-density waves (BCDW). We predict a significant thermal variation for the BCDW wavevector (in agreement with the experiments on real charge-density waves (CDWs)) unlike for analytic CDWs where the wavevector variation should be non-observable experimentally. This issue will be discussed in detail in a forthcoming paper.

In section 2, we describe some physical situations where, according to condensed matter literature, similar models appear. We will mention there some other models which, although different, can be shown to be equivalent to (1.1), regarding the mean-field properties.

In section 3, the proof of those equivalences yields a rigorous justification of the existence of a devil's staircase phase diagram at finite temperature. This result, which extends the zero-temperature characterization of the model obtained by Aubry [5], is proved under certain conditions on the model parameters.

In section 4, we explain a numerical technique based on the method of effective potentials (or zero-degree transfer matrix) [7], which allows the determination of the phase diagram of the model with no restrictions on the parameter range and arbitrary precision. We show there a sector of the phase diagram for some particular values of the model parameters. This numerical method allows a visualization of the transition mechanisms which destroy the devil's staircase scenario well outside the bounds determined in the previous section.

Section 5 is devoted to the derivation of an analytical approximation, valid for low temperatures, which gives closed expressions for some quantities of interest in some specific applications of the model, and the last section contains a summary of results and some concluding remarks regarding the applications.

2. Related models in physical systems

In a recent series of papers, a new theoretical interpretation of charge-density wave (CDW) systems [4, 2] has been developed in terms of bipolarons. The reader interested in the complete details of the theory is referred to these publications. We will briefly outline the derivation, within this theory, of the anisotropic long-range Ising model.

The bipolaronic theory has been developed in detail for the adiabatic Holstein model [8], but could be extended to many other models. We essentially assume that:

(i) The atoms are classical particles (adiabatic approximation), i.e. the quantum fluctuations of the atomic positions are assumed to be negligible with respect to the effective distortion of the lattice produced by the electronic instability [9].

(ii) The electrons are assumed to be non-interacting fermions, i.e. Coulomb repulsion is neglected, which prevents the possible formation of spin-density wave structures.

When the electronic transfer integral is set to zero, the electrons trivially localize at the sites of the lattice. At low temperature, the lattice sites either are occupied by pairs of electrons with opposite spins or are empty. These pairs of electrons, which are associated with a lattice distortion, are called bipolarons. For each site i, we introduce a pseudo-spin σ_i, which is equal to 1 if the site is occupied and 0 if the site is empty. The distribution of pseudo-spin $\{\sigma_i\}$ is arbitrary and can be random or not.

This theory establishes rigorously that, within the above hypothesis on the model, each of these bipolaronic configurations persists for a non-zero electronic transfer integral t and varies uniformly and continuously as a function of t for small enough t. A small electronic transfer integral is equivalent to a large electron–phonon coupling. It is also proven rigorously that, for small enough t, the ground state of this coupled electron–phonon model is a bipolaronic state. More exact results concerning, for example, the effect of the randomness of the lattice, of the magnetic field, etc, prove the robustness of the bipolaronic structures under many kinds of perturbations.

Numerical investigations in 1D and 2D models confirm that, for moderately large electron–phonon coupling, the ground states of electron–phonon coupled systems are already incommensurate arrays of bipolarons. This is equivalent to saying that the corresponding incommensurate structure is 'non-analytic'. It is claimed that this situation corresponds to that of all real CDWs. In addition, it has been shown for the ground state that the real lattice distortion $\{u_i\}$ is obtained by convolution of the quasi-periodic distribution of pseudo-spins $\{\sigma_i\}$ by a bipolaronic shape factor $\{b_i\}$,

$$u_i = \sum_n \sigma_n b_{i-n}. \tag{2.1}$$

This shape factor b_i decays exponentially to zero for large $|i|$ over a finite coherence length ξ. On increasing the electronic transfer integral or decreasing the electron–phonon coupling, this coherence length was found to diverge in 1D models, at some critical parameter. This transition corresponds to the TBA where the incommensurate CDW recovers its analyticity.

Since the phonon branch involved in the Holstein model is dispersionless, the interaction between the bipolarons at large electron–phonon coupling, which has been estimated in [4], originates from the overlap between the electronic wavefunctions. This interaction, which vanishes at the anti-integrable limit, is repulsive and decays exponentially. For more realistic models, the fact that the phonon branch has some dispersion introduces extra interacting terms between the bipolarons. In order to realize this fact, let us consider, for example, the following electron–phonon Hamiltonian:

$$H = -t \sum_{\langle i,j \rangle} c_i^\dagger c_j + \sum_i (\lambda u_i - \mu) c_i^\dagger c_i + \tfrac{1}{2} \sum_{i,j} M_{i,j} u_i u_j \tag{2.2}$$

where $c_i^\dagger$ and c_i are creation and annihilation fermion operators at site i of a periodic lattice at any dimension, $\langle i, j \rangle$ are neighbouring sites, u_i is the (scalar) displacement

of an oscillator at site i (the atoms are considered as classical particles), $\{M_{ij}\} = \mathsf{M}$ is the elastic matrix of the phonons, which is translationally invariant and strictly positive, λ is the electron–phonon coupling, μ is the electronic chemical potential and t is the electronic transfer integral.

The anti-integrable limit of this model is obtained for $t = 0$. Then, $n_i = c_i^+ c_i$ commutes with the Hamiltonian and the pseudo-spin σ_i is $\langle n_i \rangle = 0$ or 1. Bipolaronic eigenstates are then easily obtained for arbitrary distributions of $\sigma_i = 0$ or 1 (polaronic distributions are also available by taking some $\sigma_i = \frac{1}{2}$, but these cases are not considered in this paper; see [2] for details). At zero degrees kelvin or at low temperature, the phonon variable is eliminated by minimization over u_i, which yields

$$u_i = -\lambda \sum_n \mathsf{M}^{-1}_{i,n} \sigma_n. \tag{2.3a}$$

This equality (2.3*a*) implies (2.1) with $b_{i-n} = \mathsf{M}^{-1}_{i,n}$, which only depends on the index difference $i - n$. By substitution of this expression in (2.2), one obtains the effective spin Hamiltonian at the anti-integrable limit

$$H_{\text{eff}} = -\sum_{i,j} \tfrac{1}{2} \lambda^2 \mathsf{M}^{-1}_{i,j} \sigma_i \sigma_j - \sum_i \mu \sigma_i. \tag{2.3b}$$

It is interesting to note that this Hamiltonian does not depend on the electrons or any Fermi surface effect but only on the details of the phonon spectrum. When t increases from zero, there still exists an effective spin Hamiltonian for the bipolaronic structure, and the contribution to the spin interaction due to the overlaps of the electron wavefunctions becomes important. In real physical systems, the Coulomb interactions that were neglected in our theory of bipolarons should also contribute to the spin interaction as a repulsive term.

As a result there are several physical contributions to this pseudo-spin Hamiltonian, which are not explicitly calculable at the present stage of our study. Even if this Ising Hamiltonian were explicitly known, its ground state would not in general be explicitly calculable. There probably exist many kinds of possible ground states, commensurate, incommensurate or else with different thermal behaviour, for such Ising Hamiltonians. In any case, to understand some qualitative aspects of the thermal behaviour of bipolaronic structures, it is instructive in a first step to analyse the simplest Ising spin Hamiltonians with exactly known incommensurate ground states independently of their microscopic derivation. Hamiltonian (1.1) simply extends an exactly soluble 1D model. For the sake of simplicity we only introduce nearest-neighbour ferromagnetic interactions transversely to the chain. This choice was not motivated for physical reasons, since in real systems the interaction between the chain should rather be chosen to be antiferromagnetic. This more complicated situation should be studied later. Nevertheless, model (1.1) will already exhibit interesting and non-trivial features.

Another relevant material situation for which this anisotropic long-range interacting Ising model has been claimed to be a sensible description is the transition from neutral to ionic, experimentally observed [10] in some mixed stacked charge-transfer organic compounds as the pressure or temperature is varied. The idea goes back to Hubbard and Torrance [11], whose argument we next summarize. These materials consist of stacks of alternating donor (D) and acceptor (A) organic molecules, along

the a direction. In the ac plane the stacks are arranged in such a way that an A molecule always faces a D molecule, and so the ac plane is a checker-board arrangement of D and A molecules. On the contrary, in the b direction, ... DDD ... and ... AAA ... chains of molecules are formed.

To put the problem in its simplest terms, let us say that the electronic state of a DA pair can be either homogeneous (neutral) or ionized (D^+A^-) depending on the balance between the net ionization energy and the electrostatic Madelung energy, if other effects are assumed to be of much less importance. Owing to the spatial arrangement of the molecules, Coulomb interaction inside ac planes favours ionization of pairs, whereas along the b direction Coulomb repulsion opposes it. If the state of a pair is described by means of an Ising variable, one arrives at the formulation of a pseudo-spin Hamiltonian with ferromagnetic interaction within the ac planes and antiferromagnetic long-range interactions along the b axis. The net ionization energy term corresponds to a magnetic field. A somewhat more sophisticated model later proposed by Bruinsmaa *et al* [12] does coincide in some limit with this pseudo-spin model; these authors studied the pseudo-spin model at zero temperature, using a technique from Hubbard [13]. The inclusion in the model of thermal fluctuations (which we have considered) could enhance the ability of this appealing physical picture to explain the (still growing) set of experimental studies of the neutral-to-ionic transition.

A very similar type of modelling philosophy earlier had led Safran [14] to propose this anisotropic long-range Ising model for the understanding of staging phenomena in intercalation compounds. There the interpretation of the Ising variable is the occupancy of the intercalant sites, and the physical origin of the antiferromagnetic long-range pseudo-spin interaction is the repulsion between intercalant layers due either to the elastic strain produced by the intercalation in the host lattice, or to the possible charge donation from the intercalant atoms to the host. Within some (certainly restrictive) assumptions on the shape of the minimum-energy configurations, Safran [14] obtained some specific phase diagrams for power-law decaying long-range interactions, using a mean-field type of approach (see also Millman and Kirczenow [15]).

In the preceding situations, the appearance of the pseudo-spin model is somewhat directly connected with some long-range interacting (idealized) objects (bipolarons, donor–acceptor pairs or intercalant atoms) that describe the system. It is worthwhile mentioning here some other situations where the specific models that have been proposed to describe them are of a different type but, nonetheless, they are equivalent to the anisotropic long-range pseudo-spin model, regarding their ground states.

Certain quasi-one-dimensional magnetic systems have been modelled [16] by so-called magneto-elastic Hamiltonians, where elastic degrees of freedom (representing, for example, positions of magnetic layers) are coupled to interacting magnetic moments attached to the layers. This coupling appears explicitly in the Hamiltonian, either making the exchange interaction dependent on the interlayer distances, or making the elastic interlayer interaction dependent on the magnetic moments. Although the first choice seems to have been preferred [16], it is easily seen that both ways are equivalent in general. In the next section, concerning the process of different transformations leading to the proof of the devil's staircase, we will show the equivalence between those models and the mean-field approximation to model (1.1).

Finally, de Gennes [17] proposed a model for the stacking of molecules in discotic liquid crystals, in which each molecule has two different parts, say a plate and a

chain. Assuming some interaction potentials between (i) neighbouring plates, (ii) neighbouring chains, and (iii) plate and chain of the same molecule, one arrives at a model in which the competition between the length scales determined by (i) and (ii) could lead to modulated arrangements of molecules. The interaction potential (i) was assumed to be of Lennard-Jones type, and the model was studied in the continuum limit [17] as well as numerically [18]. If the Lennard-Jones potential used in these references is substituted by a double well, this model turns out to be equivalent to the mean-field approximation to model (1.1), as we will see. Whether such a type of potential could be of use in some particular material remains an open question.

3. The devil's staircase at finite temperature

The anisotropic long-range Ising model in a magnetic field (1.1), at zero temperature and provided a convexity condition is fulfilled (see equation (3.1) below), is equivalent to a Frenkel–Kontorova model with a piecewise parabolic potential [5]. It has been shown that the variation of the modulation wavevector, ξ, of the ground state with the magnetic field H is a complete devil's staircase (DS), i.e. (i) the curve $\xi(H)$ is continuous, (ii) for each rational value of ξ, the curve $\xi(H)$ is constant over a finite interval of width ΔH, and (iii) the sum over all rationals of the widths of these intervals is equal to the total variation in H (completeness). The convexity condition mentioned above is

$$K(n) = J(n+1) + J(n-1) - 2J(n) > 0 \tag{3.1}$$

for all n ($|n| \geqslant 2$); this is a sufficient condition for the existence of the devil's staircase. The width of the plateaux of the DS for rational commensurabilities $\zeta = r/s$ (r and s are irreducible integers) is proportional to $\sum_{p=1}^{\infty} psK(ps)$, which is positive. If the range of the interaction is truncated beyond a finite distance n_0 ($J(n) = 0$ for $|n| \geqslant n_0$), the devil's staircase $\xi(H)$ becomes a harmless staircase with only a finite number of plateaux corresponding to commensurabilities with $s \leqslant n_0$ and thus shows a finite number of jump discontinuities (although they can be rather small if n_0 is large).

Although there have been some speculations on what happens at finite temperature (see for example Bak and Bruinsmaa [5]), no answer has yet been given on the effect of thermal fluctuations on the devil's staircase in 3D models. We will address this question here for the model (1.1) within a particular mean-field approach. This type of approximation has been confirmed to give correct qualitative results in models like the 3D ANNNI model [19] for a wide range of temperatures, and we do not expect a breakdown here. The derivation of the mean-field free energy corresponding to (1.1) closely follows the one for the 3D ANNNI model (see for example [20]) and the result is

$$\Phi(\{m_i\}) = \sum_i \left(\sum_{(n>0)} J(n) m_i m_{i+n} \right) - H m_i + V(m_i) \tag{3.2}$$

where m_i ($-1 \leqslant m_i \leqslant 1$) is the thermal average magnetization per spin in layer i and the mean-field potential $V(m_i)$, given by

$$V(m) = -Jm^2 + \tfrac{1}{2} k_B T[(1+m)\ln(1+m) + (1-m)\ln(1-m)] \tag{3.3}$$

is a symmetric double well (see figure 1(*a*)) below the paramagnetic transition temperature $k_B T = 2J$. The constant J is related to the J in (1.1) by $J = 4J$. Moreover we assume the explicit form $J(n) = D\eta^{|n|}$ $(0 \leqslant \eta \leqslant 1)$ of equation (2.2) for the long-range interaction constant $J(n)$, which straightforwardly satisfies convexity condition (3.1).

We prove rigorously for η sufficiently small $(\eta < \frac{1}{4})$ that the devil's staircase behaviour, which occurs as a function of the magnetic field H, is preserved in model (3.2) at low but non-zero temperature. Although our method of proof fails when η becomes close to 1, this does not mean that the DS does not survive at low temperature. Although a numerical investigation, which necessarily has a limited

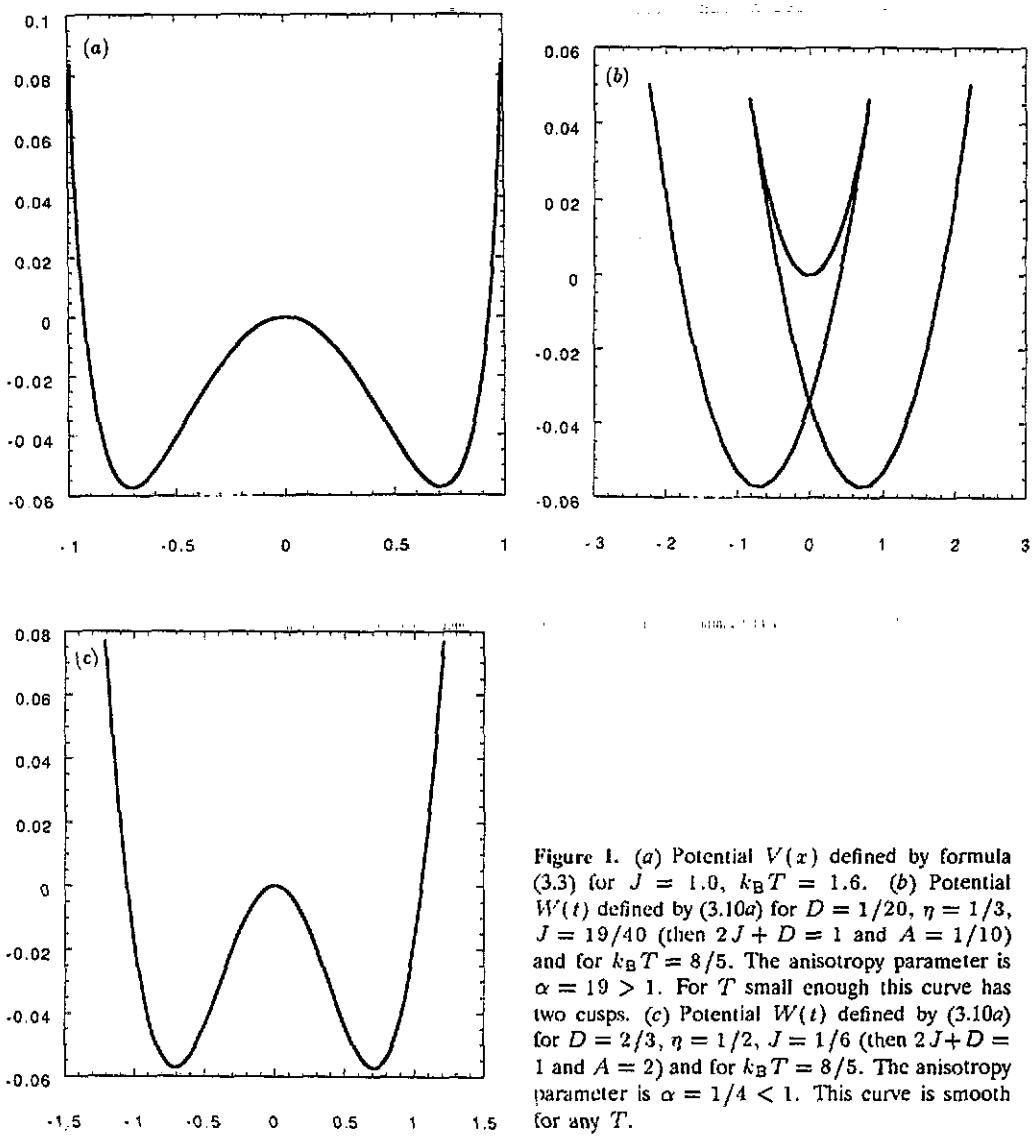

Figure 1. (*a*) Potential $V(x)$ defined by formula (3.3) for $J = 1.0$, $k_B T = 1.6$. (*b*) Potential $W(t)$ defined by (3.10*a*) for $D = 1/20$, $\eta = 1/3$, $J = 19/40$ (then $2J + D = 1$ and $A = 1/10$) and for $k_B T = 8/5$. The anisotropy parameter is $\alpha = 19 > 1$. For T small enough this curve has two cusps. (*c*) Potential $W(t)$ defined by (3.10*a*) for $D = 2/3$, $\eta = 1/2$, $J = 1/6$ (then $2J + D = 1$ and $A = 2$) and for $k_B T = 8/5$. The anisotropy parameter is $\alpha = 1/4 < 1$. This curve is smooth for any T.

accuracy, is not sufficient for proving such a conjecture when η becomes close to 1, our numerical analysis does not appear clearly in contradiction with this assumption.

The arguments used for this proof essentially consist of a series of equivalences between different models regarding their ground states. When $\eta < \frac{1}{4}$, we end in an equivalent Frenkel–Kontorova (FK) type of model with (non-parabolic) convex interactions, where the devil's staircase behaviour is well known to occur.

In appendix 1, we prove the equivalence, regarding the ground-state problem, between the model (3.2) and the following models (see section 2).

3.1. Model (A): de Gennes model

In this model

$$\Psi(\{u_i\},\{v_i\}) = \sum_i U(u_{i+1}-u_i) + \frac{C}{2}(u_i - v_i)^2 + \frac{A}{2}(v_{i+1}-v_i-b)^2. \tag{3.4}$$

This model yields model (3.2) by setting $u_{i+1} - u_i = m_i$ and minimizing over $\{v_i\}$. The potentials and the constants involved in this model are related to those of the initial model (3.2) by

$$U(m) = V(m) - \tfrac{1}{2}Dm^2 \tag{3.5}$$

$$A = D(1+\eta)/(1-\eta) \qquad C = D(1-\eta^2)/\eta \tag{3.6}$$

$$Ab = H. \tag{3.7}$$

3.2. Model (B): magneto-elastic model

Here

$$F(\{m_i\},\{y_i\}) = \sum_i \frac{C}{2}y_i^2 + \frac{A}{2}(y_{i+1}-y_i+m_i)^2 - Hm_i + \frac{A}{2}b^2 + U(m_i)$$

$$= \sum_i \frac{C}{2}y_i^2 + \frac{A}{2}(y_{i+1}-y_i-b+m_i)^2 + U(m_i) - H(y_{i+1}-y_i). \tag{3.8}$$

This model also yields model (3.2) by minimizing over $\{y_i\}$. Models (A) and (B) are directly related by setting $v_i - u_i = y_i$ and $u_{i+1} - u_i = m_i$.

The long-range interactions between the $\{m_i\}$ of the initial model (3.2) have been eliminated in both models (A) and (B) by introducing a local coupling with an additional harmonic field $\{v_i\}$ or $\{y_i\}$, which only involves nearest-neighbour interactions. Since y_i is necessarily bounded, the term $\sum_i H(y_{i+1}-y_i) = H(y_N - y_0)$ in (3.8) is a microscopic term. For an infinite system, it does not play any role in the ground-state determination and can be dropped in (3.8).

By minimizing the variational form (3.8) with respect to $\{m_i\}$, we obtain another equivalent model with only one variable per unit cell.

3.3. Model (C): model with non-convex interactions

In this model

$$\Phi(\{y_i\}) = \sum_i \frac{C}{2} y_i^2 + W(y_{i+1} - y_i - b) \tag{3.9}$$

where the symmetric potential W is defined through the following minimization:

$$W(t) = \min_x [U(x) + \tfrac{1}{2}A(x+t)^2] \qquad (-1 \leqslant x \leqslant 1). \tag{3.10a}$$

Then $\{m_i\}$ is related to $\{y_i\}$ by

$$U'(m_i) + A(m_i + (y_{i+1} - y_i - b)) = 0. \tag{3.10b}$$

Model (C) corresponds to a chain of particles in harmonic potentials, where y_i is the displacement of particle i from its equilibrium position, which are coupled by an anharmonic interaction potential that depends on the interparticle distance, $y_{i+1} - y_i - b$.

Let us examine in more detail the properties of $W(t)$. Using x as a parameter, the function $W(t)$ is the lower envelope of the possibly multivalued curve Ω parametrized by the equations

$$t(x) = -x - (1/A)U'(x) = -x - (1/A)\{-(2J+D)x + \tfrac{1}{2}k_B T \ln[(1+x)/(1-x)]\} \tag{3.11a}$$

$$W(x) = U(x) + [1/(2A)]U'(x)^2. \tag{3.11b}$$

It is easily found by differentiation that

$$\mathrm{d}W/\mathrm{d}t = -U'(x) \tag{3.12a}$$

$$\mathrm{d}^2W/\mathrm{d}t^2 = \mathrm{d}(\mathrm{d}W/\mathrm{d}t)/\mathrm{d}t = AU''(x)/[A + U''(x)] \tag{3.12b}$$

which implies that $W(t)$ and $U(x)$ are both symmetric double well ($k_B T < 2J + D$) or symmetric single well ($k_B T > 2J + D$). $W(t)$ and $U(x)$ have the same minima $W(x_0(T)) = U(x_0(T))$ at the location $t = -x = x_0(T)$, which fulfils

$$2(2J + D)x_0 = k_B T \ln[(1 + x_0)/(1 - x_0)]. \tag{3.12c}$$

However, when $W(t)$ is a double well, there are two possible situations depending on whether $t(x) = -x - (1/A)U'(x)$ is a monotonically decreasing function of x or not. When $U''(0) + A$ is negative, that is when

$$0 < 2J + D - A \tag{3.13a}$$

$$k_B T < 2J + D - A \tag{3.13b}$$

the curve Ω has two symmetric cusps and a knot (cf. figure 1(*b*)) so that the lower envelope $W(t)$ has a cusp at $t = 0$ corresponding to the knot. Conversely, when $U''(0) + A$ is positive, $W(t)$ is smooth with no cusp and knot (cf. figure 1(*c*)).

It is then useful to define the anisotropy parameter

$$\alpha = J/[D\eta/(1 - \eta)] = J(1 - \eta)/D\eta \tag{3.13c}$$

as the ratio of the total interchain coupling J and of the total intrachain coupling $\sum_{n>0} J(n)$. Then $W(t)$ has a cusp when two conditions are fulfilled: (i) the anisotropy parameter α is larger than 1; (ii) the temperature is small enough, that is

$$k_B T < 2J - 2D\eta/(1-\eta) = 2J(1-1/\alpha). \tag{3.14}$$

Let us consider now another type of model.

3.4. Model (D): Sasaki–Griffiths model

Sasaki and Griffiths [21] noted that a particular class of models with the form (3.9) can be exactly transformed into FK models. This situation is obtained when potential $W(t)$ can be written exactly as

$$W(t) = \min\{W_0(t), W_0(t+\Delta)\} \tag{3.15a}$$

where $W_0(t)$ is a strictly convex function with a minimum between 0 and Δ. Then, introducing new pseudo-spin variables $\sigma_i = 0$ or 1, the ground state $\{y_i\}$ of the variational form (3.9) is given by minimization of the variational form

$$\Phi(\{y_i\}) = \sum_i \min_{\sigma_i} \left(\frac{C}{2} y_i^2 + W_0(y_{i+1} - y_i - b + \sigma_i \Delta) \right). \tag{3.15b}$$

By setting

$$z_i = y_i + \Delta \sum_{n=0}^{i-1} \sigma_n = y_i + \Delta M_i \tag{3.16a}$$

where $M_i = \sum_{n=0}^{i-1} \sigma_n$ is an integer, this form becomes

$$\Phi(\{z_i\}) = \sum_i V_{FK}(z) + W_0(z_{i+1} - z_i - b). \tag{3.16b}$$

By dropping the condition $\sigma_i = M_{i+1} - M_i = 0$ or 1 and considering $\{M_i\}$ as arbitrary integers, this model is nothing else than a Frenkel–Kontorova model with a piecewise parabolic potential

$$V_{FK}(z) = \tfrac{1}{2} C \min_{M \text{ integer}} (z - \Delta M)^2 \tag{3.16c}$$

with period Δ and a convex potential W_0 coupling the nearest-neighbour atoms. The exact ground state of this FK model (3.16) is obtained for $M_i = \text{int}(i\zeta + \alpha)$ where α is an arbitrary phase and $0 \leqslant \zeta \leqslant 1$ since $W_0(x)$ has a minimum between 0 and Δ. Therefore, the condition $\sigma_i = M_{i+1} - M_i = 0$ or 1 is automatically fulfilled by the ground state $\{z_i\}$ of the FK model, which thus corresponds to the ground state of model (3.15). There exists a hull function $f(x) = x + g(x)$ where $g(x)$ is 1-periodic such that $z_i = f(i\zeta + \alpha)$ and $y_i = z_i + \Delta M(z_i/\Delta)$ where $M(z) = \text{int}(z + \frac{1}{2})$ is the closest integer to z.

Although the double-well potential defined by (3.10*a*) does not have the form (3.15*a*) (except at zero degrees kelvin), in some cases, it can be replaced equivalently by another double-well potential with the form (3.15*a*).

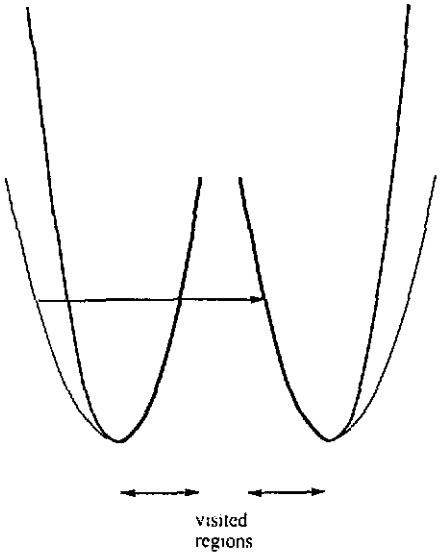

Figure 2. Sketch of the construction of potential $\tilde{W}(t)$ from potential $W(t)$.

3.5. Model (C'): variation of model (C) with the form (D)

Let us consider the symmetric potentials $\tilde{U}(x)$ and $\tilde{W}(t)$ defined as (see figure 2)

$$\tilde{U}(x) = U(x) \qquad \text{for } |x| \leqslant x_0(T)$$
$$\tilde{W}(t) = W(t) \qquad \text{for } |t| \leqslant x_0(T)$$

$$\tilde{U}(x) = U(x - 2x_0(T)) \qquad \text{for } x > x_0(T)$$
$$\tilde{W}(t) = W(t - 2x_0(T)) \qquad \text{for } t > x_0(T)$$

$$\tilde{U}(x) = U(x + 2x_0(T)) \qquad \text{for } x < -x_0(T)$$
$$\tilde{W}(t) = W(t + 2x_0(T)) \qquad \text{for } t < -x_0(T).$$

These definitions of $\tilde{X}$ potentials just correspond to replacing one part of the potential X by a translation of the remaining part (see figure 2). It is readily proven (as suggested by figure 2) that

$$\tilde{W}(t) \leqslant W(t) \tag{3.17a}$$

and

$$\tilde{U}(x) \leqslant U(x). \tag{3.17b}$$

Defining $\tilde{W}_0(t) = \tilde{W}(t)$ for $t > 0$, $\tilde{W}(t)$ can be written as

$$\tilde{W}(t) = \min\{\tilde{W}_0(t), \tilde{W}_0(t + \Delta)\} \tag{3.18a}$$

with

$$\Delta = 2x_0(T). \tag{3.18b}$$

Models (A) and (B) where potential $U(x)$ is replaced by potential $\tilde{U}(x)$ are called models (A′) and (B′) respectively. Model (C′) is obtained from model (C) by replacing $W(t)$ by $\tilde{W}(t)$ since

$$\tilde{W}(t) = \min_x [\tilde{U}(x) + \tfrac{1}{2}A(x+t)^2] \qquad (-1 \leqslant x \leqslant 1).$$

Models (A′), (B′) and (C′) are equivalent with exactly the same arguments as for models (A), (B) and (C). They also are equivalent to model (3.2)′ where potential (3.3) is replaced by $\tilde{V}(m) = \tilde{U}(m) + \frac{1}{2}Dm^2$. In the same range of temperature as for model (C), the ground state of model (C′) only 'visits' the convex part of $\tilde{W}(t)$. Consequently model (C′) with variational form

$$\Phi(\{y_i\}) = \sum_i \min_{\sigma_i} \left(\frac{C}{2} y_i^2 + \tilde{W}_0(y_{i+1} - y_i - b + \sigma_i \Delta) \right) \tag{3.19}$$

has the form of model (D) required by Sasaki and Griffiths. When the minimum, $x_0(T)$, of $\tilde{W}_0(t)$ is such that the corresponding value of $z_{i+1} - z_i$ in model (3.16), $x_0(T) + b$, satisfies

$$0 < x_0(T) + b < \Delta = 2x_0(T)$$

or

$$-x_0(T) < b = \frac{H}{A} = \frac{H}{D}\frac{1-\eta}{1+\eta} < x_0(T) \tag{3.20}$$

the exact results known about the FK model apply and the ground state $\{z_i\}$ of model (3.16) is an incommensurate structure: there exists $0 \leqslant \zeta \leqslant 1$ and a phase $0 \leqslant \alpha < 1$ such that

$$M_i = \mathrm{int}(i\zeta + \alpha). \tag{3.21a}$$

On the other hand, when $H/A > x_0(T)$, it is straightforward to show that $y_i \equiv 0$, $M_i \equiv 0$ and $\sigma_i \equiv 0$ in (3.18) yields the ground state. Then, (3.21*a*) holds with $\zeta = 0$. A similar result holds when $H/A < -x_0(T)$, which yields $\zeta = 1$ in (3.21*a*).

Thus, in all cases we have for the corresponding ground states of models (A′), (B′) and (C′)

$$\sigma_i = \mathrm{int}((i+1)\zeta + \alpha) - \mathrm{int}(i\zeta + \alpha) = \chi(i\zeta + \alpha) \tag{3.21b}$$

where

$$\chi(x) = \mathrm{int}(x + \zeta) - \mathrm{int}(x) \tag{3.21c}$$

is the characteristic function, which is 0 or 1 and periodic with period 1.

In appendix 3, we prove that, for $\eta < \frac{1}{4}$ and T small enough, the ground states of models (3.2) with potential $V(m)$ and $\tilde{V}(m) = \tilde{U}(m) + \frac{1}{2}Dm^2$ are identical. Since the second model is equivalent to a Frenkel–Kontorova model, the ground states of the initial model are commensurate or incommensurate, and the wavevector of the modulation depends on the magnetic field H as a complete devil's staircase.

For η close to 1, the method used in appendix 3 for proving the persistence of a DS at low temperature does not work. This is due to the fact that for the ground state

$\{m_i\}$ of model (3.2), there exists $|m_i|$ such that $|m_i| > x_0(T)$. Thus models (A), (B) and (C) are not necessarily equivalent to models (A′), (B′) and (C′) respectively.

Nevertheless, our numerical results suggest that the devil's staircase scenario remains valid or at least is a good approximation for any η when the temperature is low enough. In the following sections we use two different techniques for obtaining the phase diagram. The first numerical method is exact in principle, but requires longer computations for a high accuracy. It confirms this assertion within the numerical errors. The second method is analytic, but based on an approximation of $W(t)$ by a piecewise parabolic potential. It yields explicitly a phase diagram that is in agreement at low temperature with those obtained by the first method.

4. The minimization eigenvalue method

In the previous section we have proved that the ground states of the original pseudo-spin model (3.2) map exactly those of model (C):

$$\Phi(\{y_i\}) = \sum_i (C/2)y_i^2 + W(y_{i+1} - y_i - b). \tag{4.1}$$

This one can be considered as a displacement model by considering variable y_i as the displacement from the equilibrium position of the ith particle of a chain. The interparticle interactions in this chain are nearest-neighbour and double-well shaped (see figure 1).

As we have already noted, it is much easier to compute the phase diagram with model (C) than with the initial model, which involves long-range interactions. For 1D models with short-range interactions like (C), efficient numerical techniques extending the transfer matrix method at zero degrees have been developed. The method, called the effective potential method, or minimization eigenvalue method, is described in great detail in the recent review by Griffiths [7].

This method applied to model (C) consists of finding a scalar λ and a function $R(y)$ that fulfil the following functional equation:

$$R(y) + \lambda = (C/2)y_i^2 + \min_{y'}[W(y - y' - b) + R(y')]. \tag{4.2}$$

For each value of y, $y' = \tau(y)$ is defined as the value y' where the minimum in (4.2) occurs. The attractor of this (contractive) map is a ground state of the model, and λ turns out to be the ground-state energy per atom. Formally (4.2) is the continuum version of the eigenvalue problem in minimax algebras [22], λ being the (unique) additive eigenvalue and $R(y)$ the corresponding additive right-eigenfunction.

$R(y)$ can be interpreted as the effective potential, which acts on the last particle (with coordinate y) of a semi-infinite chain extending to the right-hand side, when assuming that all the other particles are relaxed in the arrangement with the lowest energy. One can define identically an effective potential $S(y)$ for a semi-infinite chain extending to the left-hand side, which fulfils

$$S(y) + \lambda = (C/2)y_i^2 + \min_{y'}[S(y') + W(y' - y - b)]. \tag{4.3}$$

With both (right- and left-) eigenfunctions, the effective potential $F(y)$ that acts on a particle of a fully infinite chain, when all the other particles on both sides are relaxed in their configuration with the smallest energy, is

$$F(y) = R(y) + S(y) - (C/2)y_i^2. \tag{4.4}$$

As shown next, this effective potential $F(y)$ gives detailed information about the ground-state properties and its low-energy excitations.

Equation (4.2) is solved by numerical procedures assuming that y belongs to a grid of N points on the interval $-y_{max} \leqslant y \leqslant y_{max}$. The maximum value y_{max} is chosen for each set of parameters in order that, for the ground state, y_i surely belongs to that interval. The number N of points in the grid can be as large as the computer capabilities and/or precision requirements suggest. We have used $N = 500$ in most cases. The interparticle potential $W(y-y'-b)$ defined implicitly by equation (3.10) is preliminarily calculated for y and y' belonging to the chosen grid.

The discretized minimization eigenvalue equation is solved by using the algorithm of minimizing cycle, explained in [23]. The algorithm yields the exact solution of the discrete eigenvalue problem in a finite time (roughly proportional to N^2). Therefore, the accuracy of the result is essentially determined by the pitch of the grid used for y.

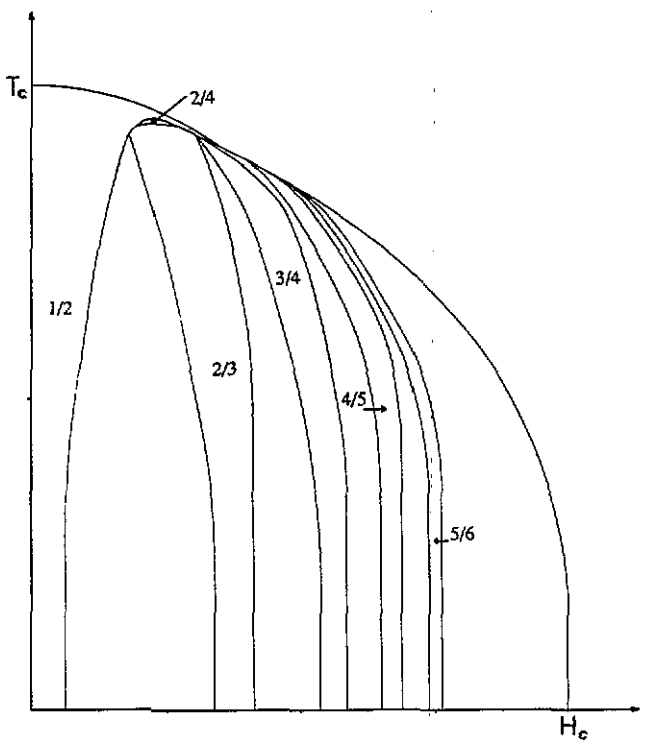

Figure 3. Phase diagram in the T–H plane (for $D = 1$, $\eta = 0.8$, $J = 0.5$), obtained by the method of effective potentials. Only the widest phases are shown, labelled by wavevector ζ. Although these values of the parameters lie well beyond the rigorous bounds we found, a devil's staircase seems to exist here up to $T \simeq 0.6T_c$. The phase labelled 2/4, which can be seen at high temperature, has period 4, but wavevector 1/2. We follow the notation of [16, 24] in order to distinguish this phase from the 'normal' 1/2 phase.

Figure 3 shows the phase diagram versus H and T for $J = \frac{1}{2}$, $D = 1$ and $\eta = 0.8$ (the anisotropy parameter (3.13) is $\alpha = \frac{1}{8}$). Modulated phases do appear in the region of the H–T plane defined by

$$k_B T < k_B T_{MF} = 2J + 2D\eta/(1+\eta)$$

(the paramagnetic transition temperature at $H = 0$)

and

$$H < H_c = 2D\eta/(1-\eta)$$

(the homogeneous-to-modulated transition field at $T = 0$).

At zero temperature, agreement with the exact result [5] is obtained, which tests the quality of the numerical codes. At low temperatures, the width of the stability domain of each modulated phase changes very little. Although $\eta > \frac{1}{4}$, the DS seems to persist at low temperature.

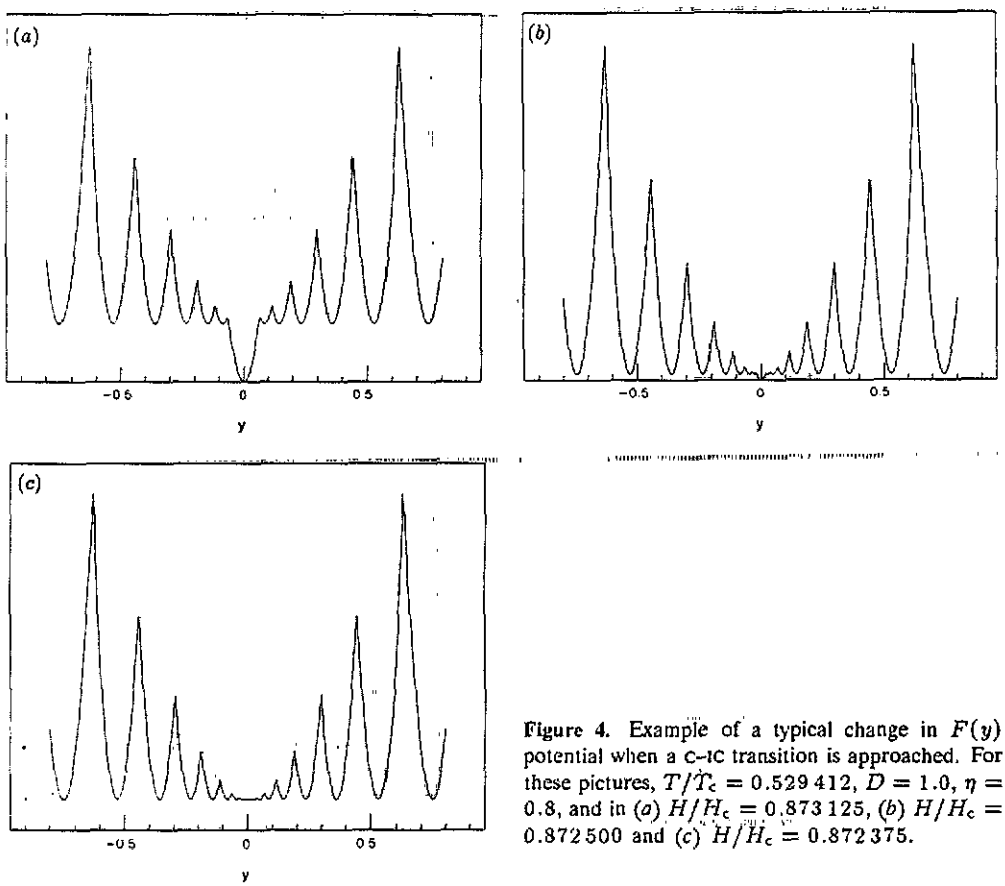

Figure 4. Example of a typical change in $F(y)$ potential when a C–IC transition is approached. For these pictures, $T/T_c = 0.529\,412$, $D = 1.0$, $\eta = 0.8$, and in (*a*) $H/H_c = 0.873\,125$, (*b*) $H/H_c = 0.872\,500$ and (*c*) $H/H_c = 0.872\,375$.

Some examples of effective potentials $F(y)$ are shown in figure 4. Function $F(y)$ exhibits absolute minima for the values y_i belonging to a ground-state configuration. It also exhibits local minima corresponding to the metastable configurations $\{y_i\}$, which are called discommensurations. The difference ΔF between these minima and the absolute minima is the energy of the discommensuration, i.e. the cost of creating such an excitation. A commensurate–incommensurate (C–IC) transition occurs when the discommensuration energy ΔF vanishes; an example of this situation is shown in the sequence of figure 4. This behaviour, which is characteristic of a devil's staircase,

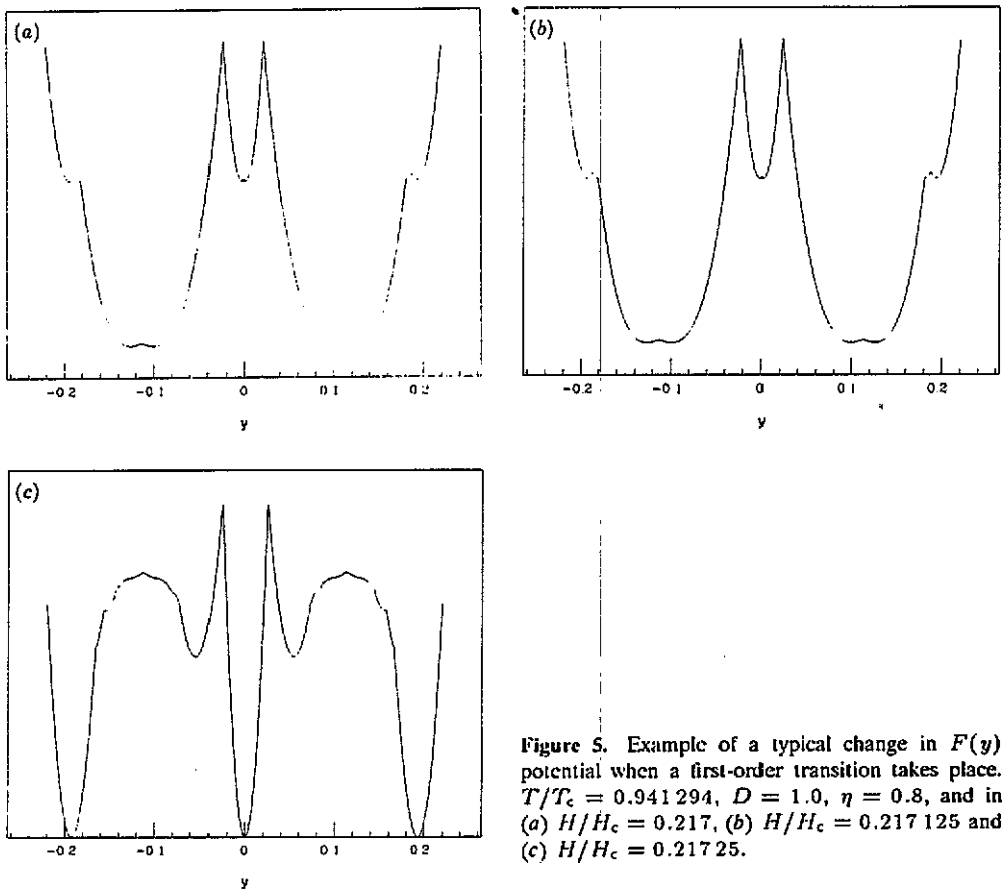

Figure 5. Example of a typical change in $F(y)$ potential when a first-order transition takes place. $T/T_c = 0.941\,294$, $D = 1.0$, $\eta = 0.8$, and in (*a*) $H/H_c = 0.217$, (*b*) $H/H_c = 0.217\,125$ and (*c*) $H/H_c = 0.217\,25$.

is numerically observed over a wide range of temperatures. It suggests that the DS survives in fact to rather large temperature.

By contrast, for larger temperatures the behaviour of $F(y)$ becomes quite different. As shown in figure 5, first-order phase transitions (i.e. discontinuous change of both the ground-state positions and the modulation wavevector) can take place before the discommensuration energy vanishes, which proves that the DS disappears at least partially. Other interesting features can be observed such as, for example, second-order phase transitions corresponding to a period doubling. Then, the modulation wavevector of a commensurate ground state changes discontinuously and is divided by 2, i.e. the unit cell doubles, while the particle positions change continuously.

However, it is well known that the mean-field approximation becomes unreliable at larger temperature where one approaches the critical line at the border of the homogeneous (paramagnetic) region. Therefore, the existence of first-order transitions and of period-doubling transitions remains questionable for the initial model (1.1).

We should mention here the resemblance of this phase diagram (figure 3) with that of the model studied by Marchand and Caillé [16], which should be clearly understood after consideration of section 3. Also, many features of this phase diagram are shared by the one of the XY chiral model studied by Yokoi *et al* [24]. Moreover, as this

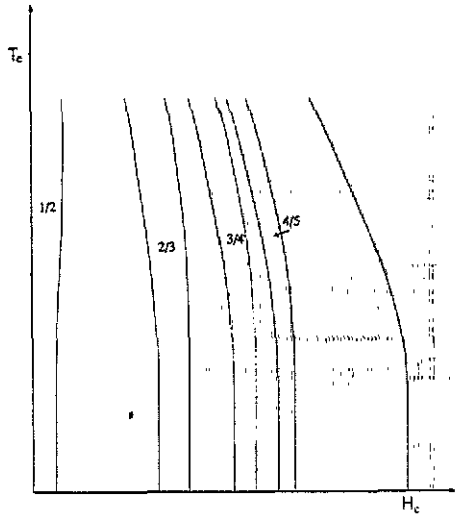

Figure 6. Phase diagram in the T–H plane for the same values of parameters as in figure 3 ($D = 1$, $\eta = 0.8$, $J = 0.5$), obtained by the parabolic approximation of potential $W(t)$ at low enough temperature. The results are quite in agreement with those of section 4, and the quantitative values are available up to $T \simeq 0.4T_c$.

paper was completed, we became aware of a recent work by Ishimura [25], in which the phase diagram for this model has been obtained by means of a 'brute force' numerical procedure, without saying clearly if the devil's staircase survives or not at low enough temperature.

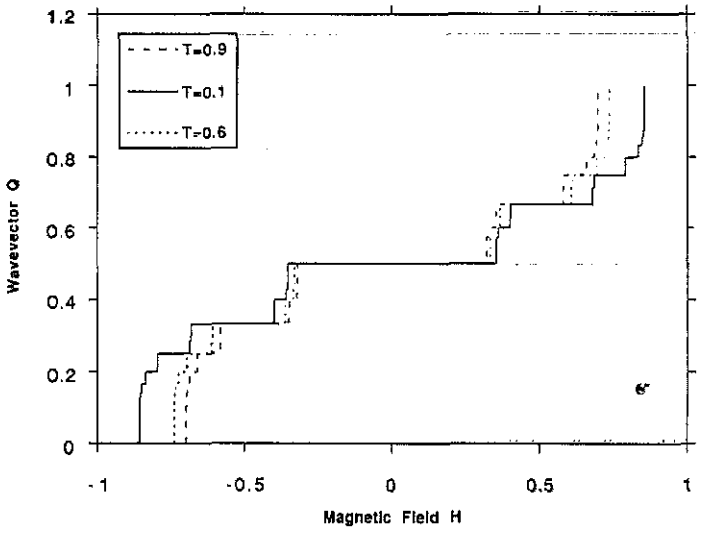

Figure 7. Phase diagram at fixed temperature in the Q–H plane, where Q is the wavevector, obtained with the parabolic approximation of potential $W(t)$. The devil's staircase is plotted for three different values of T, and for $D = 1$, $J = 0.5$, $\eta = 0.3$.

5. Low-temperature analytical approximation

In this section, we assume that the temperature is low enough in order that the ground state of model (3.9) only visits the convex part of the double-well potential

$W(t)$. Then this double well can be approximated reasonably well by a piecewise parabolic potential, allowing an explicit calculation of the phase diagram versus T and H.

We replace $W(t)$ in (3.9) by the parabolic approximation:

$$W(t) \simeq \min\left[\tfrac{1}{2}W''(x_0)(t-x_0)^2, \tfrac{1}{2}W''(x_0)(t+x_0)^2\right] + W(x_0). \tag{5.1}$$

The constant term $W(x_0)$ does not play any role in the determination of the phase diagram, and can be dropped, as we shall do in the following. The values $\pm x_0 = \pm x_0(T)$ are the two minima of the potential $U(x)$ (with $-1 < x < +1$). $W(t)$ can be written as

$$W(t) \simeq \min_{\sigma}\left\{\tfrac{1}{2}W''(x_0)[t - \tfrac{1}{2}\Delta(T) + \Delta(T)\sigma]^2\right\} \qquad \text{where } \sigma = 0 \text{ or } +1. \tag{5.2}$$

Now, we are interested in the evaluation of $W(y_{i+1} - y_i - b)$ in model (3.9). At this point, we introduce the new variables $\{z_i\}$ and $\{\sigma_i\}$, as defined in (3.16)

$$z_i = y_i + \Delta(T)\sum_{j=0}^{i-1}\sigma_j \tag{5.3}$$

and $W(y_{i+1} - y_i - b)$ becomes

$$\begin{aligned} W(y_{i+1} - y_i - b) &\simeq \min_{\sigma_i}\left\{\tfrac{1}{2}W''(x_0)[y_{i+1} - y_i - b - \tfrac{1}{2}\Delta(T) + \Delta(T)\sigma_i]^2\right\} \\ &= \min_{\sigma_i}\left\{\tfrac{1}{2}W''(x_0)[z_{i+1} - z_i - b - \Delta(T)\sigma_i - \tfrac{1}{2}\Delta(T) + \Delta(T)\sigma_i]^2\right\} \\ &= \tfrac{1}{2}W''(x_0)[z_{i+1} - z_i - b - \tfrac{1}{2}\Delta(T)]^2. \end{aligned} \tag{5.4}$$

Following this transformation, the first part of model (3.11) is also changed and becomes

$$\sum_i \tfrac{1}{2}Cy_i^2 = \sum_i \tfrac{1}{2}C[z_i - \Delta(T)M_i]^2. \tag{5.5}$$

The model (3.11) thus becomes with respect to the new variables:

$$\frac{\Psi(\{z_i\})}{W''(x_0)} = \tfrac{1}{2}\sum_i \lambda(T)\min_{\{p_i\}}[z_i - \Delta(T)M_i]^2 + \tfrac{1}{2}[z_{i+1} - z_i - b - \tfrac{1}{2}\Delta(T)]^2 \tag{5.6}$$

with

$$\lambda(T) = C/W''(x_0). \tag{5.7}$$

The model (5.6) is a piecewise parabolic Frenkel–Kontorova model, which is exactly solvable [5]. These models depend on the temperature T (through the value of $t_0(T)$). Taking the analytical result in [5], we obtain for the ground state

$$M_i = \mathrm{int}(i\zeta(T) + \alpha) \tag{5.8a}$$

$$z_i = B(T)\sum_{n=-\infty}^{+\infty}\tau(T)^{|n|}M_{i+n} \tag{5.8b}$$

$$B(T) = \Delta(T)\lambda(T)/[4\lambda(T) + \lambda(T)^2]^{1/2} \tag{5.8c}$$

$$\tau(T) = 1 + \tfrac{1}{2}\lambda(T) - \tfrac{1}{2}[4\lambda(T) + \lambda(T)^2]^{1/2} \tag{5.8d}$$

where $\mathrm{int}(x)$ denotes the integer part of x, α is the phase of the ground state, and $\zeta(T)$ is the wavevector of modulation, which is the same, by successive equivalences, as the wavevector of the models (A), (B) and (C).

The magnetic field is connected to the wavevector by

$$b = \frac{H(T,\zeta)}{A} + \frac{\Delta(T)}{2} = \frac{\Delta(T)\lambda(T)^2}{2[4\lambda(T)+\lambda(T)^2]^{1/2}} \sum_{n>0} n[2\,\mathrm{int}^{\pm}(n\zeta(T)) + 1]\tau(T)^n. \tag{5.9}$$

Using function $\tau(T)$ instead of $\lambda(T) = [1-\tau(T)]^2/\tau(T)$, the magnetic field becomes as a function of T and ζ:

$$H(T,\zeta) = D\frac{1+\eta}{1-\eta}\frac{\Delta(T)}{2}\left(\frac{[1-\tau(T)]^3}{\tau(T)[1+\tau(T)]}\sum_{n>0} 2n\,\mathrm{int}^{\pm}(n\zeta(T))\tau(T)^n - \frac{2\tau(T)}{1+\tau(T)}\right). \tag{5.10}$$

The notation $\mathrm{int}^{\pm}(x)$ denotes the two possible definitions of the integer part for x integer (i.e. $\mathrm{int}^{+}(n) = n$, and $\mathrm{int}^{-}(n) = n-1$ for n integer, and $\mathrm{int}^{\pm}(x) = \mathrm{int}(x)$ for x non-integer). This induces discontinuities for each rational value of $\zeta(T) = r/s$ (r and s being irreducible integers). At T fixed, $H(T,\zeta)$ is invertible, and the inverse function $\zeta(T,H)$ is a continuous function, known as the complete devil's staircase. For $T = 0$, we have $\pm x_0 = \pm 1$, $W''(\pm 1) = A$, and as a consequence $\tau(0) = \eta$. Thus the formula (5.10) gives

$$H(0,\zeta) = D\left(\frac{2(\eta-1)^2}{\eta}\sum_{n>0} n\eta^n\,\mathrm{int}^{\pm}(n\zeta(0)) - \frac{2\eta}{1-\eta}\right) \tag{5.11}$$

which yields the variation $\zeta(H)$ of the initial model at $T = 0$. We can expand $\tau(T)$ at low temperature, using the fact that for $t_0(T) = 1-\epsilon_0(T)$, $\epsilon_0(T) \ll 1$. In that case, we obtain

$$U'[1-\epsilon_0(T)] = 0 \simeq -2J_0 + \tfrac{1}{2}k_B T \log[2/\epsilon_0(T)] \tag{5.12a}$$

$$\epsilon_0(T) \simeq 2\exp(-4J_0/k_B T) \tag{5.12b}$$

with $J_0 = J + D/2$. Following the same approximation for $W''(t_0)$ and $\tau(T)$, we obtain

$$\lambda(T) \simeq (C/A)[1 + (2A/k_B T)\epsilon_0(T)] \tag{5.13}$$

$$\tau(T) \simeq \eta[1 - (2D/k_B T)\epsilon_0(T)]. \tag{5.14}$$

By substitution of the value of (5.8*d*) in (5.10), we can draw the DS at finite temperature T (see figure 6) and the phase diagram for some values of parameters η, D and J as shown in figure 7. At low enough temperature, this last figure is in quite good agreement with the figure obtained for the same parameters in section 4.

6. Conclusions

In summary, concerning the physical results obtained in this paper for a particular mean-field model:

(i) We have shown (and proven rigorously under extra conditions) that the complete devil's staircase that exists at zero temperature persists at non-zero temperature.

(ii) We have also shown that the temperature has an effect on the width of the tongues: this is reduced except that corresponding to commensurability $\frac{1}{2}$.

Concerning the mathematical methods used in this paper, which could find applications for other models:

(i) We have established an equivalence regarding the ground state between models with long-range interactions and models with short-range interactions. The trick consists of the introduction of an extra discrete field of variables $\{y_i\}$, which 'transport' the interaction at long distance.

(ii) By elimination of the initial field of variables $\{m_i\}$, we have shown under some conditions that the model becomes equivalent to a Frenkel–Kontorova model.

For finding explicitly the phase diagram with a good accuracy, we performed two approaches, which are in good qualitative agreement with one another (in the low-temperature regime). The first one is the minimization eigenvalue method, which is in principle exact, but with an accuracy that depends numerically on the pitch of a grid. The second method uses the approximation of potentials by piecewise parabolic functions, which yields analytic calculations and remarkably accurate results at low temperature.

The 3D model studied in this paper consists of incommensurate chains coupled ferromagnetically. In a short forthcoming paper, it will be shown that, when fixing the magnetization of the model (which corresponds to fixing the number of electrons if this model is used for a *bipolaronic charge-density wave*), we necessarily have a significant variation of the wavevector of the modulation as a function of temperature. This variation is thermally activated and, although it has the wrong sign, it exhibits unusual locking effects at simple commensurabilities and striking similarities with unexplained features observed on real CDWs. However, for describing more precisely real CDWs, an antiferromagnetic coupling between the chains would be more realistic and could give results in better agreement with experiments. The method used here cannot be used identically for solving this modified model. Modified methods are under study.

Acknowledgments

We would like to acknowledge R B Griffiths for his interest and helpful comments. LMF and PQ want to express their gratitude to, respectively, the Laboratoire Léon Brillouin and the Universidad de Zaragoza for their kind hospitality. Financial support from DGICYT (PB89/054), Action Integrée Franco–Espagnole (HF-057) and EEC project SCI*/0229-C (AM) are acknowledged.

Appendix 1.

Minimization of (3.8) with respect to $\{y_i\}$ gives, for all n,

$$A(m_n - m_{n-1}) + (C + 2A)y_n - A(y_{n+1} + y_{n-1}) = 0. \tag{A1.1}$$

These equations can be solved using a Fourier transform:

$$u_n = \sum_q u(q)\exp(-iqn) \qquad y_n = \sum_q y(q)\exp(-iqn) \tag{A1.2}$$

which yields

$$y(q) = [\![A(1 - e^{iq})/\{C + 2A[1 - \cos(q)]\}]\!]m(q). \tag{A1.3}$$

By substitution of $y(q)$ into the variational form (3.8), one obtains

$$\min_{\{y_i\}} \Phi(\{m_i\},\{y_i\}) = \tfrac{1}{2}AC\sum_q \frac{m(q)m^*(q)}{C + 2A[1 - \cos(q)]} = \sum_i \left(\sum_{n>0} J(n)m_i m_{i+n}\right) + \tfrac{1}{2}Dm_i^2 \tag{A1.4}$$

which establishes the equivalence between model (B) and the original model (3.2).

Appendix 2.

We prove that, for low enough temperature, the set of values taken by $t_i = y_{i+1} - y_i - b$ for the ground state of model (3.9) lie in the convex part of the potential $W(t)$, i.e. $W''(t_i) > 0$ for all i.

Proof. The derivatives of $V(x)$ are $V'(x) = -2Jx + \frac{1}{2}k_B T \ln[(1 + x)/(1 - x)]$ and $V''(x) = -2J + k_B T/(1 - x^2)$. Since for $x > 0$, $V''(x)$ is a monotonically increasing function that diverges for $x \to +1$, the symmetric potential $V(x)$ is a double well when $V''(0) < 0$, that is for

$$k_B T < 2J. \tag{A2.1}$$

Then, $V(x)$ has two minima at $x = \pm x_1(T)$, such that $V'(x_1) = 0$ and $V''(x_1) > 0$, which implies $V''(x) \geqslant V''(x_1) = V''(-x_1) > 0$ for $|x| \geqslant x_1(T)$. It is more convenient to consider $0 \leqslant x_1 < 1$ as the variable instead of T. Then, we have

$$k_B T(x_1) = 4Jx_1/\ln[(1 + x_1)/(1 - x_1)]. \tag{A2.2}$$

For the ground-state configuration $\{m_i\}$, the variational form (3.2) is an absolute minimum with respect to each m_i. The part of (3.2) that only depends on m_i has the form $V(m_i) - h_i m_i$ with

$$h_i = H - \sum_{n\neq 0} J(n)m_{i+n} \tag{A2.3}$$

which yields

$$V'(m_i) = h_i. \tag{A2.4}$$

Since $V(x)$ is a symmetric double well, m_i has the sign of h_i and

$$|m_i| \geqslant x_1(T) \tag{A2.5}$$

which implies

$$V''(m_i) \geqslant V''(x_1) > 0. \tag{A2.6}$$

We now consider $U(x) = V(x) - (D/2)x^2$. Thus we have

$$U''(m_i) = V''(m_i) - D \geqslant U''(x_1) = V''(x_1) - D. \tag{A2.7}$$

We obtain

$$\begin{aligned} U''(x_1) &= -(2J + D) + k_B T 1/(1 - x_1^2) \\ &= -(2J + D) + [4Jx_1/(1 - x_1^2)]1/\ln[(1 + x_1)/(1 - x_1)]. \end{aligned} \tag{A2.8}$$

Condition $U''(x_1) > 0$ is equivalent to $F(x_1) = 4Jx_1 - (2J+D)(1-x_1^2)\ln[(1+x_1)/(1-x_1)] > 0$. It is easy to check that $F''(x_1) > 0$ for $0 \leqslant x < 1$, which implies that $F(x_1)$ is convex. Since $F(0) = 0$, $F'(0) = -2D < 0$, $F(1) = 4J > 0$, the set of positive $U''(x_1)$ is a unique interval $]x_{1m}, 1[$. Consequently for $T < T_m = T(x_{1m})$, any ground-state configuration $\{m_i\}$ of model (3.2) fulfils $U''(m_i) \geqslant U''(x_1) > 0$ and thus only visits the convex part of $U(x)$.

The ground-state configuration $\{y_i\}$ of model (3.9) is related to $\{m_i\}$ through the equality

$$U'(m_i) + A(m_i + t_i) = 0 \tag{A2.9}$$

with

$$t_i = y_{i+1} - y_i - b \tag{A2.10}$$

and (3.12*b*) yields

$$W''(t_i) = AU''(m_i)/[A + U''(m_i)] > 0$$

which proves that, at low enough temperature, the ground state $\{y_i\}$ of model (C) only visits the convex part of potential $W(y_{i+1} - y_i - b)$.

Appendix 3.

We prove that, for $\eta < \frac{1}{4}$ and for low enough temperature, the ground states of models (3.2) with potential $V(m)$ and $\tilde{V}(m) = \tilde{U}(m) + \frac{1}{2}Dm^2$ are identical.

Proof. The proof is obtained by showing that we have $|m_i| \leqslant x_0(T)$ for the ground state $\{m_i\}$ of model (3.2) with potential $\tilde{V}(m)$. Then, we have for all i, $\tilde{V}(m_i) = V(m_i)$. Because of the inequalities (3.17), which imply $\tilde{V}(m) \leqslant V(m)$, the ground states of model (3.2) with potential $V(m)$ and $\tilde{V}(m)$ are the same.

Let us consider model (3.2) with potential $\tilde{V}(m)$. Since this model is equivalent to a FK model, the ground state $\{m_i\}$ is described by a 1-periodic hull function $m(x)$ as

$$m_i = m(i\zeta + \alpha). \tag{A3.1}$$

The sign of m_i is determined by the equality

$$\operatorname{sgn}(m_i) = 1 - 2\sigma_i \tag{A3.2}$$

where $\sigma_i = \chi(i\zeta + \alpha)$ is defined by the hull function (3.21*b*). Consequently, we can write

$$m(x) = [1 - 2\chi(x)]\tfrac{1}{2}[1 + x_1(T)][1 + \epsilon(x)] \tag{A3.3}$$

where the hull function $\epsilon(x)$ fulfils, because of (A2.5),

$$|\epsilon(x)| < [1 - x_1(T)]/[1 + x_1(T)]. \tag{A3.4}$$

The local field $h_i = h(i\zeta + \alpha)$ defined by (A2.3) can also be written with a hull function $h(x)$ defined as

$$h(x) = H - \sum_{n\neq 0} J(n)m(x + n\zeta) = [1 + x_1(T)] \sum_{n\neq 0} J(n)\chi(x + n\zeta)$$
$$+ \left(H - \tfrac{1}{2}[1 + x_1(T)] \sum_{n\neq 0} J(n) \right) + r(x) \tag{A3.5}$$

with

$$r(x) = \tfrac{1}{2}[1 + x_1(T)] \sum_{n\neq 0} J(n)[1 - 2\chi(x + n\zeta)]\epsilon(x + n\zeta)$$

and

$$|r(x)| < \tfrac{1}{2}[1 - x_1(T)] \sum_{n\neq 0} J(n) = [1 - x_1(T)]D\eta/(1 - \eta). \tag{A3.6}$$

Let us consider the function

$$\phi(x) = \sum_{n\neq 0} J(n)\chi(x + n\zeta) = \sum_{n\neq 0} J(n)[\operatorname{int}(x + (n + 1)\zeta) - \operatorname{int}(x + n\zeta)]$$
$$= -J(1)[\operatorname{int}(x + \zeta) - \operatorname{int}(x)] + \sum_{n=1}^{\infty} [J(n) - J(n + 1)][\operatorname{int}(x + (n + 1)\zeta)$$
$$- \operatorname{int}(x - n\zeta)]$$

and the difference between its maximum and minimum

$$0 < \max_x \phi(x) - \min_x \phi(x) < J(1) \max_x [\operatorname{int}(x + \zeta) - \operatorname{int}(x)] - \min_x [\operatorname{int}(x + \zeta)$$
$$- \operatorname{int}(x)] + \sum_{n=1}^{\infty} [J(n) - J(n + 1)] \left(\max_x [\operatorname{int}(x + (n + 1)\zeta) \right.$$
$$\left. - \operatorname{int}(x - n\zeta)] - \min_x [\operatorname{int}(x + (n + 1)\zeta) - \operatorname{int}(x - n\zeta)] \right). \tag{A3.7}$$

Function $[\operatorname{int}(x + (n + 1)\zeta) - \operatorname{int}(x - n\zeta)]$ is 1-periodic with two discontinuities with amplitudes 1 and -1 per period. Thus,

$$\max_x [\operatorname{int}(x + (n + 1)\zeta) - \operatorname{int}(x - n\zeta)] - \min_x [\operatorname{int}(x + (n + 1)\zeta) - \operatorname{int}(x - n\zeta)] = 1 \tag{A3.8}$$

which implies

$$0 < \max_x \phi(x) - \min_x \phi(x) < J(1) + \sum_{n=1}^{\infty} [J(n) - J(n+1)] = 2J(1) = 2D\eta. \tag{A3.9}$$

Consequently, using (A3.5) we have

$$0 < \max_x h(x) - \min_x h(x) < 2[1 - x_1(T)]D\eta/(1-\eta) + 2[1 + x_1(T)]D\eta = \rho(T). \tag{A3.10}$$

Since for an incommensurate structure $h(x)$ takes both positive and negative values (see appendix 2), the right-hand side $\rho(T)$ of (A3.10) is an upper bound for the local field h_i. For T going to zero, $x_1(T)$ goes to 1 and this upper bound goes to $4D\eta$. Note that $\rho(T)$ is an increasing function of T. When $4D\eta < D$, that is for $\eta < \frac{1}{4}$, there exists T_m such that for $T < T_m$ we have for all i, $h_i \leqslant \rho(T) < D$. Then comparing (A2.4), $V'(m_i) = h_i$, and the equation $V'(x_0(T)) = Dx_0(T)$, it comes out that for all i we have $|m_i| < x_0(T)$.

References

[1] Aubry S, Gosso J-P, Abramovici G, Raimbault J-L and Quémerais P 1991 *Physica* D **47** 461

[2] Aubry S, Abramovici G and Raimbault J-L 1991 *J. Stat. Phys.* submitted

[3] In the *anti-integrable limit*, the discrete-time dynamical system whose trajectories correspond to stationary configurations (of the model under consideration) reduces to a Bernouilli shift; thereafter the name *coding sequence* for the (formal) representation of a configuration in that limit. Both concepts, *anti-integrable limit* and *coding sequence*, as well as others, are explained in:
Aubry S and Abramovici G 1990 *Physica* D **43** 199–219
Aubry S 1992 *Proc. IMA Workshop on Twist Mappings and their Applications* (Minneapolis, 1990) at press

[4] Aubry S and Quémerais P 1989 *Low-Dimensional Electronic Properties of Molybdenum Bronzes and Oxides* ed C Schlenker (Dordrecht: Kluwer) pp 295–405
Quémerais P 1987 *PhD Thesis* Université de Nantes, France
Quémerais P and Raimbault J-L 1990 *Eur. J. Solid State Inorg. Chem.* **27** 503

[5] Aubry S 1978 *Solitons and Condensed Matter Symp. (Oxford)* ed A R Bishop and T Schneider; *Solid State Sciences* **8** 264–78
Aubry S 1983 *J. Phys. C: Solid State Phys.* **16** 2497
Bak P and Bruinsmaa R 1982 *Phys. Rev. Lett.* **49** 249 for a different approach

[6] Vallet F, Schilling R and Aubry S 1986 *Europhys. Lett.* **2** 815–22; 1988 *J. Phys. C: Solid State Phys.* **21** 67–105

[7] Griffiths R B 1990 *Fundamental Problems in Statistical Mechanics VII* ed H van Beijeren (Amsterdam: Elsevier) pp 69–110

[8] Holstein T 1959 *Ann. Phys., NY* **8** 325

[9] The effect of quantum fluctuations has been considered in:
Aubry S and Quémerais P 1989 *Singular Behavior and Nonlinear Dynamics* ed S Pnevmatikos, T Bountis and S Pnevmatikos (Singapore: World Scientific) pp 342–63
Aubry S, Abramovici G, Feinberg D, Quémerais P and Raimbault J-L 1989 *Nonlinear Coherent Structures (Lecture Notes in Physics 353)* ed M Barthes and J Leon (Berlin: Springer) pp 103–16
Aubry S, Quémerais P and Raimbault J-L 1990 *Proc. 3rd Eur. Conf. on Low Dimensional Conductors and Superconductors* ed S Barisić; *Fisica* **21** Suppl. 3, 98–101
Raimbault J-L 1990 *PhD Dissertation* Université de Nantes, France

[10] Torrance J B, Vazquez J E, Mayerlee J J and Lee V Y 1981 *Phys. Rev. Lett.* **46** 253
Torrance J B, Girlando A, Mayerlee J J, Crowley J A, Lee V Y, Batail P and Laplaca S J 1981 *Phys. Rev. Lett.* **47** 1747

[11] Hubbard J and Torrance J B 1981 *Phys. Rev. Lett.* **47** 1750
[12] Bruinsmaa R, Bak P and Torrance J B 1983 *Phys. Rev.* B **27** 456
[13] Hubbard J 1978 *Phys. Rev.* B **17** 494
[14] Safran S A 1980 *Phys. Rev. Lett.* **44** 937
[15] Millman S E and Kirczenow G 1982 *Phys. Rev.* B **26** 2310
[16] Marchand M and Caillé A 1988 *Phys. Rev.* B **38** 4845
[17] de Gennes P G 1983 *J. Physique Lett.* **44** 657
[18] Godreche C and de Seze L 1985 *J. Physique Lett.* **46** 39
[19] Selke W 1992 *Phase Transitions and Critical Phenomena* ed C Domb and J L Lebowitz (New York: Academic)
Selke W 1988 *Phys. Rep.* **170** 213
Yeomans J 1988 *Solid State Phys.* **41** 151
[20] Yokoi C S O, Coutinho-Filho M D and Salinas S R 1981 *Phys. Rev.* B **24** 4047
[21] Sasaki K and Griffiths R B 1988 *J. Stat. Phys.* **53** 1031
[22] Cunninghame-Greene J 1979 *Minimax Algebra* (Berlin: Springer)
[23] Floría L M and Griffiths R B 1989 *Numer. Math.* **55** 565
[24] Yokoi C S O, Tang L H and Chou W 1988 *Phys. Rev.* B **37** 2173
[25] Ishimura N 1991 *J. Phys. Soc. Japan* **60** 2051